A conjugate study of the polar ionospheric F2-layer and IRI-2007 at 75° magnetic latitude for solar minimum

HE Fang[1*], ZHANG BeiChen[1], Joran Moen[2] & HUANG DeHong[1]

[1]SOA Key Laboratory for Polar Science, Polar Research Institute of China, Shanghai 200136, China;
[2]Department of Physics, University of Oslo, Norway

Abstract   Long-duration conjugate observations by the EISCAT Svalbard Radar (ESR) and the ionosonde at Zhongshan station from the International Polar Year (IPY) during solar minimum conditions are analyzed, with respect to variability in the F2-layer peak parameters. A comparison between International Reference Ionosphere-2007 (IRI-2007) and observation data clearly demonstrates good agreement in summer, but greater deviations in winter. The IRI model reproduces the F2 peak parameters dominated by solar photoionization reasonably well, but it does not address the effect of electron precipitation. Hence, the discrepancies become large in the winter auroral ionosphere.

0 Introduction

The ground-based sounding is important for continuously monitoring ionosphere-magnetosphere coupling in the polar region. During the 2007–2008 International Polar Year (IPY), observation instruments such as the European Incoherent Scatter Radar (EISCAT), the Super Dual Auroral Radar Network (SuperDARN), and digital ionosondes were coordinated to investigate the polar ionosphere. Efficient exchange of data between the participants gave an excellent opportunity to study the polar space environment. The joining of the Chinese to the EISCAT radar association extends opportunities for continued conjugate observations.

The International Reference Ionosphere (IRI) model[1−2] is widely used in ionospheric research. IRI is an empirical model based on global observation data. Given geographic location, date and time, it provides altitude profiles of electron density, electron temperature, ion density and ion temperature, from 50–1 500 km. Because of the complicated structure of the polar ionosphere, non-uniform distribution of ionosonde stations, and limited data coverage, comparative studies of the IRI model and observation data have mainly focused on the mid-low latitude region[3−5]. There have been some validation studies of the IRI model for polar regions, using EISCAT radar or satellite observations[6−9]. In general, however, there is better agreement with observations in mid and low latitudes than in high latitude polar cap regions. As asserted by Moen et al.[9], the IRI model does not represent the transport of F-region plasma across the polar cap from the EUV production region on the

*Corresponding author (email: hefang@pric.gov.cn)

dayside.

The motivation of the present paper is to validate the IRI-2007 model, using conjugate observations from Longyearbyen, Svalbard and the Zhongshan stations during solar minimum conditions. We take advantage of the IPY long run of the EISCAT Svalbard Radar (ESR) and the DPS-4 ionosonde at Zhongshan station, to compare diurnal and seasonal variations in the $F2$ layer critical frequency with the IRI-model. The paper is organized as follows. Section 1 introduces the conjugate observation instruments and data in both hemispheres. Section 2 configures the input parameters for the IRI-2007 model. Section 3 presents the comparison of the conjugate observations and IRI model. In the discussion of Section 4, we try to explain the physical processes underlying the model discrepancies. Finally, further work on IRI-2007 is suggested in the conclusions.

1   Instruments

Zhongshan station, located at 69.4°S, 76.4°E in geographic coordinates, corresponding to 77.2° magretic latitude (MLAT), was equipped with a DPS-4 ionosonde in 1995. Zhongshan station crosses 12:00 magnetic local time (MLT) at 10 universal time (UT) and 15 local time (LT). Based on long-term observation, a series of studies focusing on the Antarctic ionosphere have been carried out by Chinese researchers[10−15]. For the conjugate observation during the IPY, the ionosonde at Zhongshan station performed a long duration observation of 331 effective days. The sampling rate was 5 min.

The geographic coordinates of the ESR are 78.15°N and 16.05°E, corresponding to 75.27° MLAT, which make the radar suitable for conjugate studies with the Zhongshan ionosonde. The ESR operated on 285 effective days during the IPY. For ESR, we use 15 min averages of the $F2$ region maximum density ($N_{\mathrm{m}}F2$) and altitude $h_{\mathrm{m}}F2$ diurnal profiles from the 42 m antenna. We selected simultaneous observations from both ESR and the DPS-4 ionosonde on 122 days from 4 months (one month from each season). The data periods are shown in Table 1. $N_{\mathrm{m}}F2$ data obtained from the ESR were transformed to f_0F2 by

$$f_0F2 = \frac{e}{2\pi}\sqrt{\frac{N_{\mathrm{m}}F2}{\varepsilon_0 m_{\mathrm{e}}}} \tag{1}$$

where e is the electron charge; ε_0 is the vacuum permittivity; and m_{e} is the electron mass.

Table 1   Analysis dataset

		Spring	Summer	Autumn	Winter
ESR	$N_{\mathrm{m}}F2$ $h_{\mathrm{m}}F2$	2007.3	2007.6	2007.9	2007.12
DPS-4	f_0F2 $h_{\mathrm{m}}F2$	2007.9	2006.12	2007.3	2007.6

2   IRI-2007 setup

The input parameters for IRI-2007 are given in Table 2. The monthly median values from the IRI model are generated by the same technique as the observation data, which predicts 24 values at integral points for each day in the month in which the monthly median value was generated.

3   Observation results

Using the techniques introduced in the previous section, f_0F2 and $h_{\mathrm{m}}F2$ diurnal variations of ESR are shown in Figures 1 and 2; the variations of f_0F2 and $h_{\mathrm{m}}F2$ from the DPS-4 ionosonde are shown in Figures 3 and 4. The quartile difference is introduced as the error function, which indicates the median value of the data greater or less than the median value of the entire data bin.

3.1   Comparison of ESR observation and IRI model

Figure 1 compares the measured f_0F2 (from ESR) with the IRI predicted value. Figure 1a shows f_0F2 diurnal variations measured by ESR in the spring equinox month peaks around 4.2 MHz, occurring at 09 UT (10 LT/12 MLT). This peak is higher than the IRI maximum of

Table 2 IRI-2007 input parameters

	Geographic coordinate	Time period	Height range/km
ESR	78.15°N, 16.03°E	2007.3, 2007.6, 2007.9, 2007.12	86–686 (step: 2 km)
DPS-4	69.40°S, 76.40°E	2007.3, 2007.6, 2007.9, 2007.12	86–686 (step: 2 km)

3.9 MHz at local noon. The measured f_0F2 hovers above the IRI model curve, with a larger discrepancy from the daytime sector to the pre-midnight sector. For the autumn equinox month plotted in Figure 1c, a f_0F2 peak of 4 MHz occurred around 13 UT (14 LT/16 MLT), which is very close to the IRI maximum, but delayed by 2 hours. Notably, the discrepancy was smaller near the autumn equinox month than the spring equinox. Figure 1b shows the f_0F2 diurnal variation in summer month observed by ESR, agrees well with the IRI prediction, except between
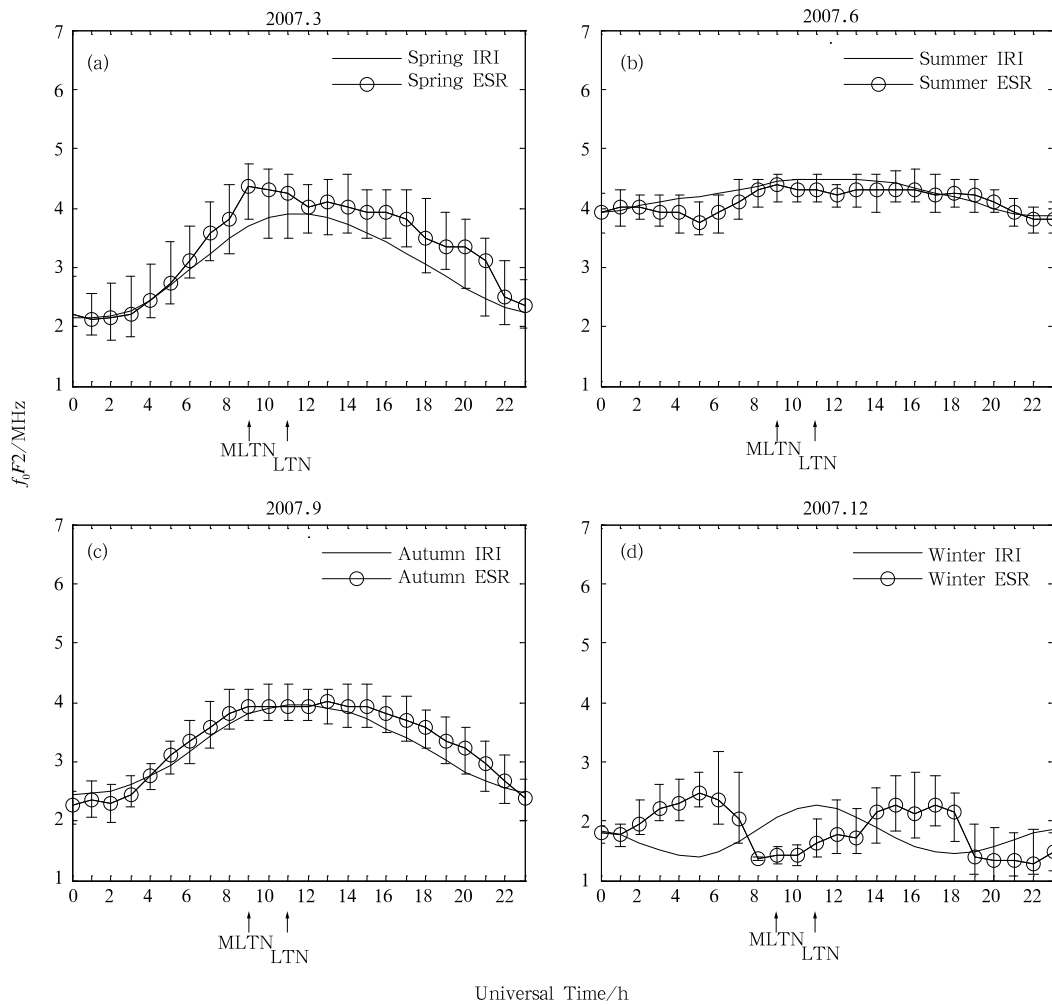

Figure 1   Diurnal variation of f_0F2 monthly median value of ESR observation and IRI prediction in different seasons (error bars indicate quartile difference).

03–07 UT (04–08 LT/06–10 MLT) in the morning sector. In winter, the f_0F2 diurnal variation observed by ESR is in anti-phase with the IRI prediction, which will be discussed in detail in Section 4.

Figure 2 compares the measured h_mF2 (from ESR) with predicted values. Figure 2b shows that the summer h_mF2 observed by ESR remained at an almost constant altitude of 230 km between 11–16 UT (12–17 LT/14–19 MLT), and 250 km between 19–09 UT (20–10 LT/22–12 MLT). The diurnal variations of h_mF2 are similar in

spring and autumn. The minimum value of 230 km was reached near geographic noon, between 11–13 UT (12–14 LT/14–16 MLT) in spring and 12–13 UT (13–14 LT/15–16 MLT) in autumn. The average altitude in spring is higher than in autumn. There is another local minimum between 05–06 UT (06–07 LT/08–09 MLT), which is 15 km higher than the main valley. The IRI h_mF2 is systematically higher than the observed value, and the largest discrepancy occurs during the polar winter.
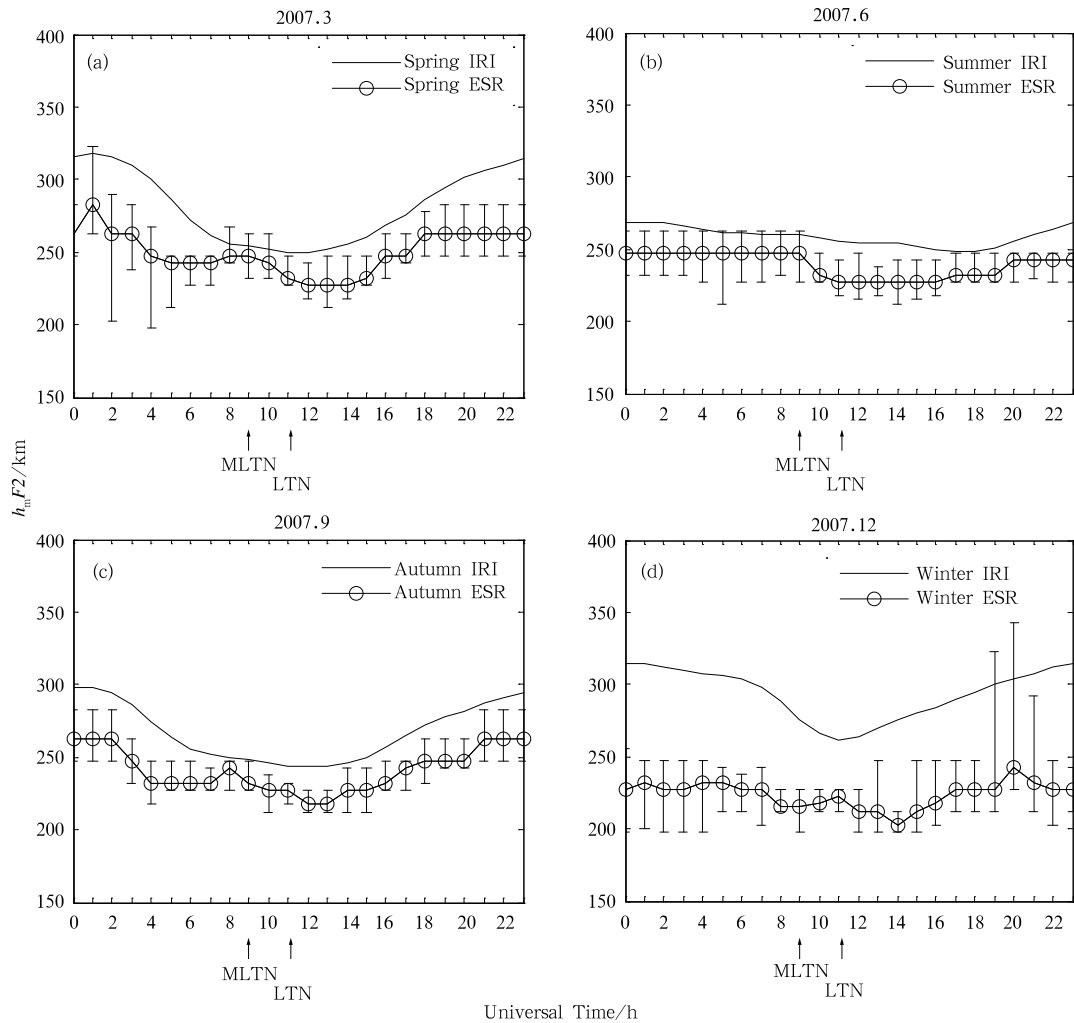

Figure 2   Diurnal variation of h_mF2 monthly median values of ESR observation and IRI prediction in different seasons.

3.2   Comparison of DPS-4 observation at Zhong-
   shan station and IRI model

Figure 3 compares the measured f_0F2 at Zhongshan with the IRI predicted values. Figure 3a shows that f_0F2 diurnal variation in the summer at Zhongshan had a max-

imum of 5.3 MHz around 07 UT (12 LT/09 MLT), which is local noon, and a minimum of 4 MHz around 20 UT (01 LT/22 MLT). The measured f_0F2 hovers near the IRI model curve. The f_0F2 maximum value at Zhongshan was 1.1 MHz higher than in Longyearbyen, and the diurnal variation scope at Zhongshan was greater,
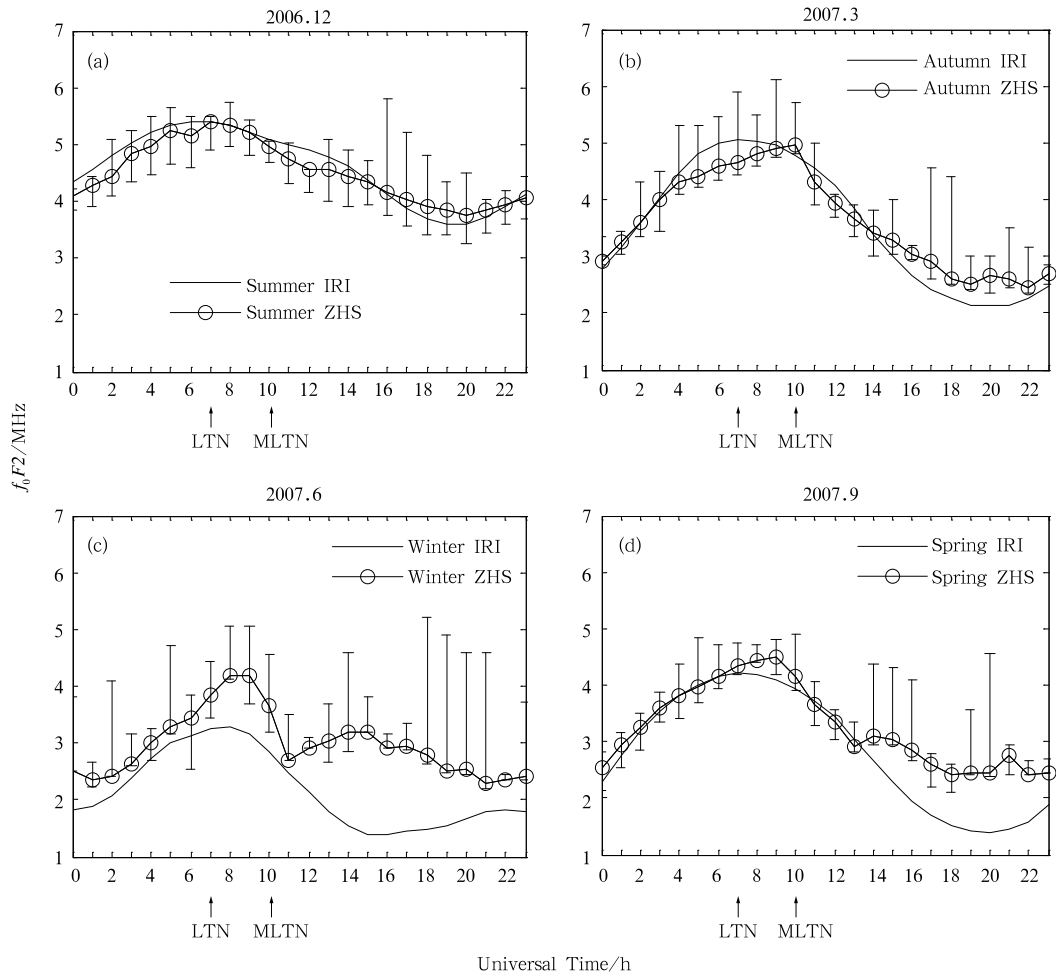
Figure 3 Diurnal variation of f_0F2 monthly median value from the DPS-4 at Zhongshan station and IRI prediction, in different seasons.

because of the difference in geographic latitude of 8.8°.

Figure 3d depicts f_0F2 diurnal variations at Zhongshan at the spring equinox month with the peak of 4.5 MHz, which occurred at 09 UT (14 LT/11 MLT). This peak is greater than the IRI maximum of 4 MHz that occurred at local noon. For the autumn equinox month (Figure 3b), a f_0F2 peak of 5.0 MHz occurred at 10 UT (15 LT/12 MLT). This peak is very close to the IRI maximum, but delayed 3 hours, i.e., it shifted from local noon to magnetic local noon. Notably, the observed f_0F2 values at night are systematically greater than the IRI model predictions, and the discrepancies were larger near the spring equinox than the autumn equinox. Figure 3c demonstrates that the IRI model underestimates the winter f_0F2 throughout the day. The measured maximum value is 4 MHz around 9 UT (14 LT/11 MLT), in contrast to the IRI model value of 3 MHz at local noon.

There is another pronounced peak around 3 MHz, near 15 MLT. As will be discussed later, the relative importance of particle impact ionization is greatest in winter.

Figure 4 compares the measured h_mF2 at Zhongshan with predicted values. In general, the measured $F2$ layer peak altitude is lower than the predicted altitude. There is much closer agreement with the IRI predictions at Zhongshan (largely within the error bars) than at Svalbard.

4 Discussion

It is clear from the observations of Section 3 that the IRI model matches the observations of the polar ionosphere during solar minimum conditions much better in summer than in winter. This indicates that the IRI model performs well when solar EUV ionization dominates. In
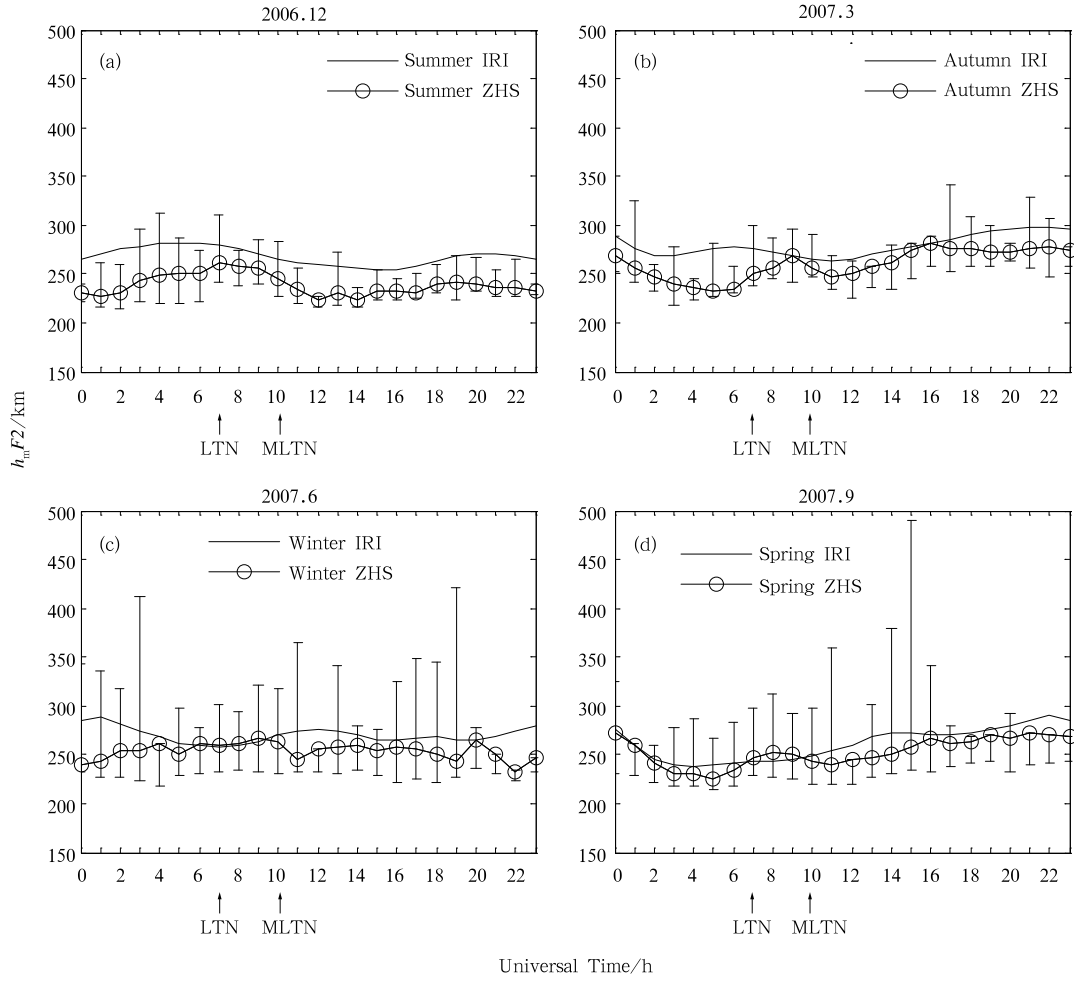
Figure 4   Diurnal variation of $h_{\mathrm{m}}F2$ monthly median value from the DPS-4 at Zhongshan station and IRI prediction, in different seasons.

this section, we discuss the physical processes that can explain the discrepancies between the model and observations. To quantify seasonal variations of these discrepancies, we introduce the mean absolute deviation (σ_1) and the standard deviation (σ_2), expressed as

$$f_0F2 \begin{cases} \sigma1 = \frac{1}{24}\sum |(\Delta f_0F2)_{\mathrm{i}}| & (2) \\ \sigma2 = \sqrt{\frac{1}{24}\sum [(\Delta f_0F2)_{\mathrm{i}}]^2} & (3) \end{cases}$$

$$f_{\mathrm{m}}F2 \begin{cases} \sigma1 = \frac{1}{24}\sum |(\Delta h_{\mathrm{m}}F2)_{\mathrm{i}}| & (4) \\ \sigma2 = \sqrt{\frac{1}{24}\sum [(\Delta h_{\mathrm{m}}F2)_{\mathrm{i}}]^2} & (5) \end{cases}$$

where Δf_0F2 and $\Delta h_{\mathrm{m}}F2$ are the differences between the observation and IRI prediction.

Comparing Figures 1 and 3, we note that the daytime f_0F2 maximum at Zhongshan is larger than at Longyearbyen for all seasons. In addition, the difference between the daytime f_0F2 maximum and the nighttime f_0F2 maximum is greater at Zhongshan than at

Longyearbyen as expected. This is because of the $\sim 10°$ difference in geographic latitude and its resultant effect on solar EUV ionization. In winter, solar EUV ionization is nearly absent above Longyearbyen, and hence the signature of particle impact ionization alone should be most pronounced at the ESR in this season. Figure 1d shows that the IRI model data are in anti-phase with the winter ESR observations. The observed f_0F2 curve has one maximum in the morning, between 04–06 UT (07–09 MLT), and there is another broad region in the afternoon with a peak between 14–18 UT (17–21 MLT). This is most likely due to the radar beam crossing a contracted auroral oval. A similar dayside f_0F2 anomaly in winter also appears at high latitudes in austral summer[20]. The value around 09 UT (12 MLT) is very low, indicating either that the ESR was located south of the cusp precipitation, or that cusp precipitation did not contribute
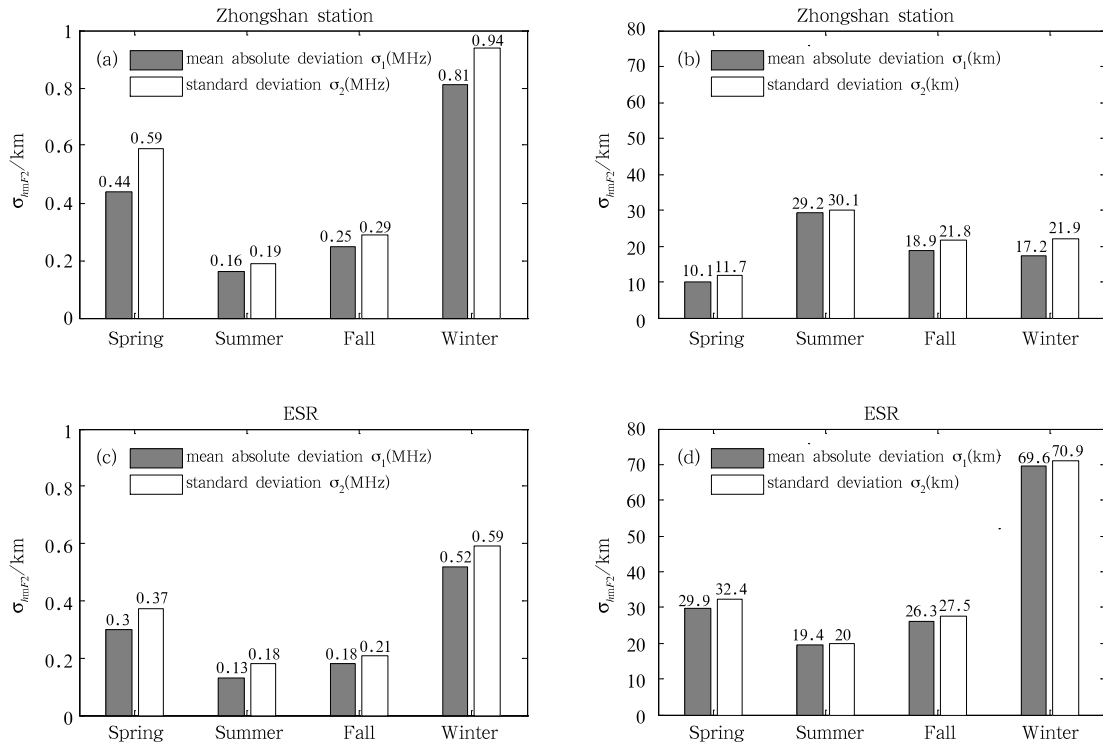
Figure 5   Deviations between IRI f_0F2 and h_mF2 predictions, and observations of the ESR at Longyearbyen and of the DPS-4 at Zhongshan station.

much to the electron density. There is a local maximum around 12 UT (15 MLT). Previous statistical analyses[16−19] indicate that there are three high-incidence areas of auroral precipitation within the auroral oval, one of which is around 15 MLT, 75° geomagnetic latitude, in proximity to the observatories at Zhongshan and Longyearbyen. Zhongshan encounters the "afternoon hotspot" region near 13 UT(15 MLT). In the Zhongshan data of Figure 3a, there is a small local maximum around 13 UT (15 MLT). There is a pronounced local maximum in winter and spring, between 14–15 UT (16-17 MLT) (Figures 3c and 3d). Later crossing indicates a more contracted polar cap.

Moen et al.[9] reported that deviations between the IRI model and ESR observations under solar maximum conditions were caused by the transport of solar EUV ionized plasma. In fact, theoretical calculations and modeling[21−22] have revealed that the observed effects may also be a consequence of the thermospheric wind system. This wind system induces a vertical ionospheric downward drift from 09:00–18:00 LT, and is responsible for the daytime decrease of f_0F2 in the aforementioned regions.

Regarding the f_0F2 peak around noon, there is a prominent offset from geographic noon to magnetic local noon in the spring ESR dataset (Figure 1a), and in the autumn and spring dataset from Zhongshan (Figures 3b and 3d). There are many factors that influence h_mF2 in polar regions, especially the neutral wind and E×B drift[23]. However, since recombination decreases with altitude, there is a simple rule of thumb to discriminate between local production within the radar beam and plasma transport through the beam: If the f_0F2 local maximum corresponds to the h_mF2 local minimum, it indicates that local plasma production dominates. For the cases above, however, the f_0F2 maxima near noon did not correspond with the h_mF2 minima, indicating that the radar beam was situated outside the production peak while observing the f_0F2 maxima. This indicates that plasma transport of solar EUV ionized plasma around magnetic noon is indeed an important factor[9]. In general, the higher the altitude of h_mF2, the longer the transport time away from the production region. For winter at Zhongshan, and autumn and spring at both stations, there are elevated f_0F2 values around magnetic midnight (19–20 UT at Longyearbyen and 20–21

UT at Zhongshan station). This indicates that plasma transport across the pole is also an issue during solar minimum conditions, but is less pronounced than during solar maximum conditions[9].

5　Conclusion

We have taken advantage of the IPY operation of the ESR and the DPS-4 ionosonde at Zhongshan station, for conjugate measurements of the $F2$ region ionosphere at 75 MLAT. This is a unique data set for solar minimum conditions. We have used this dataset to study seasonal and diurnal variation features of f_0F2 and h_mF2, and have compared those with IRI-2007 model prediction.

The IRI model agrees very well with summer observations when solar EUV ionization dominates over particle impact ionization through the day. The poorest agreement was for ESR at Longyearbyen during the polar night, when solar EUV ionization is low and particle impact ionization is the dominant ionization source. Then, crossing of the auroral oval in the morning and evening sectors becomes evident. No prominent signature of cusp precipitation is found.

For the case when both solar EUV and particle impact ionization are important, the largest discrepancies occurr in spring at both stations, and in winter at Zhongshan station. This is from the effect of plasma transport around magnetic noon and magnetic midnight, and from crossing of the auroral oval in the afternoon sector, both of which are key dynamic features of the polar ionosphere not represented by the model.

For h_mF2, agreement between prediction and observation at Zhongshan station in the southern hemisphere is superior to the agreement for ESR in the northern hemisphere.

References

1　Bilitza D. International Reference Ionosphere 2000. Radio Sci, 2001, 36: 261–275

2　Bilitza D, Reinisch B. International Reference Ionosphere 2007: Improvements and new parameters. Adv. Space Res, 2008, 42(4): 599–609

3　Lei J, Liu L, Wan W, et al. Comparison of the first long-duration IS experiment measurements over Millstone Hill and EISCAT Svalbard radar with IRI-2001. Advances in Space Research, 2006, 37: 1102–1107

4　Bertoni F, Sahai Y, Lima W L C, et al. IRI-2001 model predictions compared with ionospheric data observed at Brazilian low latitude stations. Annales Geophysicae, 2006, 24: 2191–2200

5　Zhang S, Holt J M, Bilitza D K, et al. Multiple-site comparisons between models of incoherent scatter radar and IRI. Advances in Space Research, 2007, 39: 910–917

6　Liu Y C, Ma S Y, Cai H T. The background ionospheric profiles at polar cusp latitudes-ESR observations. Chinese Journal of Polar Research, 2005, 17: 193–202

7　Cai H T, Ma S Y, Schlegel K. Climatologic characteristics of high-latitude ionosphere-EISCAT observations and comparison with the IRI model. Chinese Journal of Geophysics, 2005, 48: 471–479

8　Liu H, Stolle C, Watanabe S, et al. Evaluation of the IRI model using CHAMP observations in polar and equatorial regions. Advances in Space Research, 2007, 39: 904–909

9　Moen J, Qiu X C, Carlso H C, et al. On the diurnal variability in $F2$-region plasma density above the EISCAT Svalbard radar. Annales Geophysicae, 2008, 26: 2427–2433

10　Liu R Y, He L S, Qian S L. Ionosphere data collection at Zhongshan station in Antarctica: 1995–1999. Shanghai: Shanghai Scientific and Technological Literature Publishing House, 2000, ISBN: 7900306587

11　Liu R Y, He L S, Preliminary observation results of digital ionosonde at Zhongshan station in Antarctica. Progress in Geophysics, 1997, 12: 109–118

12　He L S, Liu R Y, Liu S L, et al. Overall properties of F region around solar minimum at Zhongshan Station, Antarctica. Chinese Journal of Geophysics, 2000, 43: 289–295

13　Zhang B C, Liu R Y, Liu S L. Simulation study on the influences of the precipitating electrons on the polar ionosphere. Chinese Journal of Geophysics, 2001, 44: 311–319

14　Xu Z H, Liu R Y, Liu S L, et al. Variations of the ionospheric F2 layer critical frequency at Zhongshan Station, Antarctica. Chinese Journal of Geophysics, 2006, 49: 1–8

15　Zhu A Q, Zhang B C, Huang J Y, et al. Comparative study of winter polar ionospheric $F2$ layer in both hemispheres. Chinese Journal of Polar Research, 2008, 20: 31–39

16　Newell P T, Lyons K M, Meng C I. A large survey of electron acceleration events. Journal of Geophysical Research (Space Physics), 1996, 101(A2): 2599–2614

17　Newell P T, Lyons K M, Meng C I. Erratum: A large survey of electron acceleration events. Journal of Geophysical Research (Space Physics), 1996, 101(A9): 19941–19942

18 Liou K, Newell P T, Meng C I, et al. Synoptic auroral distribution: A survey using polar ultraviolet imagery. Journal of Geophysical Research (Space Physics), 1997, 102(A12): 27197–27206

19 Liou K, Newell P T, Meng C I, et al. Dayside auroral activity as a possible precursor of substorm onsets: A survey using polar ultraviolet imagery. Journal of Geophysical Research (Space Physics), 1997, 102(A9): 19835–19844

20 Perevalova N P, Polyakova A S, Zalizovski A V. Diurnal variations of the total electron content under quiet helio-geomagnetic conditions. Journal of Atomspheric and Solar-Terrestrial Physics, 2010, 72: 997–1007

21 Kohl H, King J W. Atmospheric winds between 100 and 700 km and their effects on the ionosphere. Journal of Atmospheric and Terrestrial Physics, 1967, 29: 1045–1062

22 Pirog O M, Polekh N M, Chistyakova L V. Longitudinal variation of critical frequencies in polar F-region. Advances in Space Research, 2001, 27: 1395–1398

23 Rishbeth H. Thermospheric winds and the F-region: A review. Journal of Atmospheric and Terrestrial Physics, 1972, 34: 1–47